Coversheet

Title
A review of last interglacial sea-level proxies in the eastern Mediterranean coastal region

Authors

Barbara Mauz, Department of Geology and Geography, University of Salzburg, Salzburg, 5020, Austria

Noureddine Elmejdoub, Higher Institute of Water Sciences and Techniques, University of Gabès, 6072, Zrig, Gabès, Tunisia

This is a non-peer reviewed preprint submitted to EarthArXiv. An earlier version of this manuscript was submitted to *Earth System Science Data*, Special Issue "*WALIS – the World Atlas for Last Interglacial Shorelines*", edited by A Rovere et al. It was reviewed and subsequently withdrawn by the corresponding author (B Mauz). For reference see https://doi.org/10.5194/essd-2020-357.

A review of last interglacial sea-level proxies in the eastern Mediterranean coastal region

Barbara Mauz[1,2], Noureddine Elmejdoub[3]

[1]School of Environmental Sciences, University of Liverpool, Liverpool, L69 7ZT, UK
[2]Department of Geology and Geography, University of Salzburg, Salzburg, 5020, Austria
[3] Higher Institute of Water Sciences and Techniques, University of Gabès, 6072, Zrig, Gabès, Tunisia

Correspondence to: Barbara Mauz (mauz@liverpool.ac.uk)

Abstract. Mediterranean 'raised beaches' were subject to Quaternary research since the early years of the 20th century. The uniqueness of a warm-loving molluscs fauna immigrating into the Mediterranean made the coastline a prime interest for studying Quaternary sea-level changes. Today, we have a detailed picture of this historically important coastline characterised by tectonically dormant coastal zone alternating with zones that are subject to tectonic deformation. As part of the Word Atlas of last interglacial shorelines (WALIS) database we compiled 10 MIS 5e proxies for the eastern Mediterranean area available at http://doi.org/10.5281/zenodo.4454553 (Mauz, 2020). These datapoints are sea-level indicators of variable quality situated between 0±1 m and 12±10 m resulting in a reconstructed MIS 5e palaeo-sea level situated between 0±2 m and 13±10 m.

1 Introduction

The eastern Mediterranean area (Fig. 1) is a remain of the western Neotethys Ocean (Hafkenscheid and Spakman, 2006) which formed when the Indian Ocean gateway closed during the Miocene (Bialik et al., 2019). It contains the oldest oceanic crust on earth (Granot, 2016) which is actively subducting beneath the Aegean Sea (Crete, Peleponnese peninsula) and the Ionian Sea (Calabria). The oceanic crust is part of the northeast moving African plate and the continental part of this plate is a passive continental margin. The coasts of the eastern Mediterranean are therefore situated on earth's crustal segments that are, on late Quaternary time scales, actively deformed, slowly deformed or dormant. Because the eastern Mediterranean has a long history of geoscientific work the actively deformed areas, such as the Gulf of Corinth, Crete and Cyprus are very well studied (e.g., McPhee and Hinsbergen, 2019; McNeill et al., 2018). These studies used, amongst other features, the relatively well-preserved last interglacial (LIG) marine terraces. On the other side, the coast of the African passive continental margin received attention through Quaternary scientist who aimed, in the first instance at least (e.g.,

Gignoux 2013), to carry forward the biostratigraphy of the late Tertiary owing to the fauna-rich coastal deposits. Today, our understanding of the geodynamics (e.g., Nocquet, 2012) enables us to attribute the eastern Mediterranean coastal zones to large-scale geological structures (Fig. 1). This in turn enables us to separate shoreline data generated to unravel tectonic processes from sea-level data generated to reconstruct the LIG sea level and the associated ice volumes, eustacy and related GIA processes.

In this paper we describe previously published sea-level proxies on the basis of standards first developed by van de Plassche (1986) and Shennan, (1986) and recently updated in Shennan et al. (2015).

1.1 Literature overview

The overview follows the clockwise spatial arrangement of large-scale geological structures in the eastern Mediterranean (Fig. 1) starting in the north. For the sake of clarity, we use names of eastern Mediterranean sub-basins supported by names of nations. In terms of time we review literature which studied the "Tyrrhenian", a Mediterranean chronostratigraphic stage of the late Pleistocene that broadly encompasses the MIS 5 stage (Gibbard and Cohen, 2008). Historically, the Tyrrhenian stage has been identified on the basis of the so-called "Senegalese" fauna (Gignoux, 1913) which is an assemblage of warm-loving, shallow marine molluscs originating from the tropical Atlantic with the gastropod *Strombus bubonius* being its leading fossil. The Senegalese fauna immigrated into the Mediterranean during MIS 5 and disappeared with average sea-surface temperatures falling below 20°C (Sessa et al., 2013). Therefore, the assemblage disappeared most probably ~115 ka, but may have remained until ~80 ka in niches along the warm north African coast.

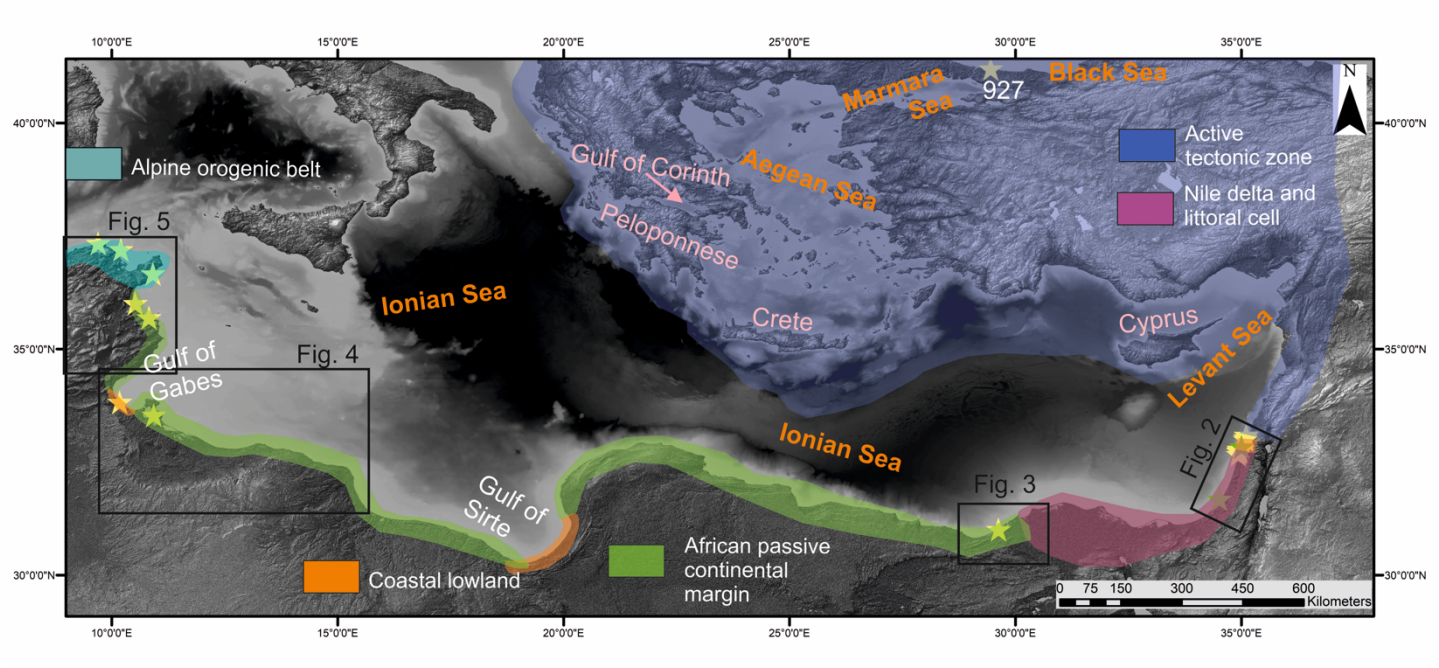

Fig. 1. The eastern Mediterranean and its coastal zones established for the purpose of this review. The zones are delimited according to the dominant geodynamic regime associated with the closure of the Tethys ocean (e.g., McPhee and van Hindsbergen, 2019), the African passive continental margin (Nocquet, 2012), the zone affected by the Nile discharge (Emery and Neev, 1960; Davis et al., 2012) and the morphological lowlands which are graben or rift basins with minor or absent tectonic activity during the late Quaternary. The Gebco data were obtained from GEBCO Compilation Group (2020) GEBCO 2020 Grid (doi:10.5285/a29c5465-b138-234d-e053-6c86abc040b9). SRTM data were obtained from http://srtm.csi.cgiar.org (Jarvis et al., 2008).

1.1.1 Active tectonic zone

Black Sea (Turkey) – this area is connected to the Aegean Sea through the ~100 m deep Bosporus sill. The Turkish Black Sea coast is in most places affected by tectonic uplift of up to 5 mm/a with the exception of the Sile site where several mm/a subsidence seems to prevail (Avsar et al., 2017). The GIA contribution to vertical land movements is estimated to ~0-1 mm/a (Avsar et al., 2017). Erginal et al. (2017) describes a shell-rich sandstone ("coquinite") at Sile situated within today's beach zone and dated to around 128 ka.

Ionian Sea (Peloponnese peninsula, Greece) – this area is situated adjacent to the Hellenic trench and the Kephalonia fault both being part of the Hellenic subduction zone. Athanassis and Foutoulis (2013) identify MIS 5 shell-rich littoral deposits on a "platform" with a palaeo-shoreline situated at ca 40 - 60 m altitude.

Ionian Sea (Corinth Gulf, Greece) – the gulf is a marginal sea connected to the Ionian Sea through two 50-60 m deep sills. It is affected by high to very high extension rates and associated uplift of coastal zones. A suite of marine terraces occurs on the southeast coast of the Gulf (Vokha plain) which attracted many researchers owing to the large number of terrace levels (16 terraces; de Gelder et al., 2019), their well-preserved topographic expression and coastal sediment cover. The early studies focused on the relationship between sea-level highstands and terrace elevation (e.g., Keraudren and Sorel, 1987; Collier, 1990) followed by studies looking at the terraces, their sediment cover and associated ages and at structural implications with the seminal paper published by Armijo et al. (1996). The researchers' interest focused on the understanding of the Corinth rift (e.g., Gawthorpe et al., 2018) and we refer the reader to De Gelder et al. (2019) for the most recent study of the terraces and to McNeill et al. (2018) for the interplay between rifting, sediment routing, climate and sea level.

Marmara Sea (Turkey) – this is a marginal sea connected to the Aegean Sea through a ca 70 m deep sill (Dardanelles). Two major branches of the North Anatolian fault (NAF) delimit the Marmara basin to the north and south forming the Marmara transtensional basin (Jenkins et al., 2020). The northern NAF strand creates deep tectonic depressions separated by structural highs (Jenkins et al., 2020). High rates of NAF motion (~20

mm/a) progressively increasing westward (Bulkan et al., 2020) and associated earthquakes makes the area a prime subject of hazard studies. Studying Pleistocene marine terraces in this area aims therefore at determining uplift rates and, in addition, the hydrodynamic history between the Black Sea and the Aegean Sea. Yaltirak et al. (2002) studied the marine terraces along the Dardanelles coast and finds the LIG terrace at 38-22 m and at 9-0 m.

Aegean Sea (Crete, Greece) – the Crete island is a subaerial forearc above the Hellenic subduction zone and thus, its shoreline-related features are used to study the geodynamics of the eastern Mediterranean (e.g., Robertson et al., 2019). The studies focus on the south coast of the island where the LIG marine terrace is situated at 116-45 m altitude (Robertson et al., 2019) and at 50-100 m altitude (Gallen et al., 2014). For the most recent study of the terraces see Ott et al. (2019) and references therein.

Levant Sea (Cyprus, Greece; Turkey) – the Cyprus island is situated above the Cyprean subduction zone. Similar to Crete, its marine terraces and related shoreline features are in the focus of structural geologists in order to understand the geodynamics of the eastern Mediterranean (e.g., McPhee and van Hinsbergen, 2019). Pleistocene deposits were studied by Vita-Finzi (1990; 1993), Zomeni (2012), Poole et al. (1990) and Poole and Robertson, (1991) with the latter two studies showing that the "Tyrrhenian" terrace is situated at <3m on the south coast. On the north coast Galili et al. (2016) find the LIG terrace at 12-17 m while Palamakumbura et al. (2016) find the same terrace at 4 m altitude.

Levant Sea (Turkey, Syria, Lebanon) – the northernmost part of the Levant coast (Turkey) is part of the collision zone between the northward moving Arabian Plate, the westward moving Anatolian Plate and the southward moving African plate. There, Tari et al. (2018) studied marine terraces occurring within the Antakya Graben and find the MIS 5e marine terrace at around 50 m altitude. Further south the coast is situated on the west flank of the sinistral Dead Sea transform fault characterised by coastal mountain ranges, pull-apart basins and graben (Brew et al., 2001). The coastal ranges are bounded by numerous normal and strike slip faults which are a consequence of the branching Dead Sea transform fault (Lebanese Restraining Bend; e.g., Weinberger et al., 2009). Dodonov et al. (2008) studied marine terraces on the Syrian coast and assigned the ones situated at 20 - 30 m to MIS 5. The southern boundary between deformed and dormant coastal zone is represented by the Rosh Hanikra fault (Morhange et al., 2006).

***Ionian Sea (north Tunisia*)** – the northernmost coast of Tunisia is part of the Alpine orogenic belt and associated tectonic processes. LIG deposits are part of cliff sections (Sahli et al., 2019) or marine terraces. Elmejdoub and Jedoui (2009) show that in NE Tunisia the LIG deposits are part of a marine terrace at ~25 m altitude.

1.1.2 Nile littoral cell and Nile delta

***Levant Sea* (*Israel*)** – The central ("Carmel") coast is part of the passive continental margin of the African plate which moves southward along the Dead Sea transform fault (e.g., Weinberger et al., 2009). It receives its sediments exclusively through the Nile littoral cell (e.g., Davis et al., 2012) which is a persistent easterly-driven longshore current created by the interplay of winds and Coriolis force. Coastal deposits bearing *Strombus bubonius* were first described by Issar and Kafri, (1972) and subsequently defined as "Yasaf" member by Sivan et al. (1999). LIG deposits occur on the Carmel coast at -1 m up to 7 m (Galili et al., 2007; 2018) and on the Sharon coast at around – 55 m (Porat et al., 2003).

1.1.3 African passive continental margin

***Ionian Sea* (*Egypt*)** – the coast sits on the African plate with minor to negligible effects from tectonic movements on the LIG deposits. The coastal plain west of the Nile delta exhibits a series of beach ridges first described and dated by El-Asmar 1994 and later by El-Asmar and Wood (2000) and studied by Elshazly et al. (2019). The second ridge behind the modern coastline was attributed to MIS 5e.

***Ionian Sea* (*Libya*)** – The coast from west of Alexandria (Egypt) to east of Tripoli (Libya) is under-studied and Quaternary deposits are only known from Explanatory Booklet provided in association to geological maps. Therein, Hinnawy and Cheshitev (1975) describe the "Gargaresh Formation" of "Tyrrhennian" age which forms an elongated ridge parallel to the modern shoreline.

***Ionian Sea (Tunisia*)** –the coast is situated on the largest eastern Mediterranean shelf. Around Djerba island the LIG coastal environment is represented by a barrier stretching from Sabratah to the southern Gulf of Gabès (Fig. 4; Jedoui et al., 2003). A barrier also existed north of the Gabès gulf in the Gulf of Hammamet and along the south coast of Cap Bon. Coastal deposits were first systematically described by Paskoff and Sanaville (1983). Hearty (1986) provide the first age for the Monastir site (Fig. 5) through his seminal work on amino acid razemisation correlated to U-series ages. Subsequently, Queslati (1994) and Jedoui et al. (2003) studied the LIG deposits on the south coast situated at 2-6 m altitude. Later, Mauz et al. (2009) studied sedimentological details of the deposits and their ages.

1.1.4 Coastal lowlands

These coastal zones are morphological lowlands. Ongoing subsidence during the Quaternary is possible but not everywhere evident from data.

Haifa bay, Rosh Hanikra platform (Levant Sea, Israel) - the northern coast is situated between the Rosh Hanikra fault and the Carmel fault. The Ahihud fault separates the Rosh Hanikra platform from Haifa bay. LIG deposits occur on the sediment-starved Galilee coast at elevations 1-2 m (Sivan et al., 2016), in Haifa bay at around -25 m (Fig. 2; Avnaim-Katav et al., 2012). No onshore coeval deposit is reported from this bay (Zviely et al., 2006).

***Gulf of Sirte* (*Libya*)** – the gulf is part of a Cretaceous rift basin undergoing northward tilting and associated subsidence (van der Meer and Cloetingh, 1993). Giglia (1984) describes shallow marine oolitic limestone situated at around 3 m around 20 km inland.

***Gulf of Gabès* (*Tunisia*)** – the gulf is part of the collapsed Jeffara block dominated by normal faulting during the Quaternary (Gharbi et al., 2014). Shape and geometry of the gulf funnels the tidal wave with the consequence that the gulf coast experiences not only the highest tidal range in the Mediterranean (MHHW 2 m; Gzam et al 2016) but also unusual shore-parallel hyrodynamic conditions (Sammari et al., 2006; Gzam et al 2016). The LIG deposit is part of a beach ridge stretching parallel to the modern coastline at ca 3 m altitude (Gzam et al., 2016).

2 Sea-level indicators

Occurrence and preservation of sea-level indicators on the eastern Mediterranean coast is controlled by the morphology, sediment supply and geological structure of the particular coastal zone as well as by the human demand for coastal resources. Large zones of coast are deprived of indicators, e.g. the frequently cited zone at Monastir (Tunisia; e.g., Kopp et al., 2009). On rocky, sediment-starved coasts erosional indicators such as abrasion platforms and tidal notches prevail while on soft sediment coasts with sufficient sediment supply beach ridges, sandy beaches, barriers and spits prevail. Sediment-starved coasts show abiotic carbonate crusts and lithophaga borings or biotic, reef-like constructions generated by red algae (corallinacea), algal serpulids, coral (Cladocora caespitosa) or vermetids. Some of the indicators can provide small vertical uncertainties, for instance, if the living range of a particular fauna is small or if the sediment facies is well constrained in terms of water depth. The most important indicators are listed in Table 1.

Table 1. RSL proxies mentioned in the text. For description of tidal regime see section 3.

Name of RSL indicator	**Description of RSL indicator**	**Description of RWL**	**Description of IR**	**Indicator reference(s)**
Marine terrace	Flat, gently seaward dipping rock surface bearing a veneer of coastal sediment and/or fauna, typical for sediment-starved coasts	(Storm wave swash height + Breaking depth) / 2	Storm wave swash height - Breaking depth	Rovere et al. (2016)
Sediment facies	Beach: gently seaward dipping planar laminae of (bioclastic, carbonate, siliciclastic) sand or pebbly sand; poor to moderate sorting, landward coarsening of grain size	(MHHW + MTL)/2	backshore to upper foreface (ca +0.5 m to -0.0 m water depth)	Miall (2010); Reading (1986); Shennan et al. (2015)
Sediment facies	Foreshore: plane beds, low-amplitude symmetrical bedforms, parallel laminae or foresets, bioturbated beds of (bioclastic, carbonate, siliciclastic) sand, moderate sorting, seaward fining of grain size	(MTL+LAT)/2	Upper foreshore to upper shoreface (ca 0.0 m to -0.5 m)	Miall (2010); Reading (1986); Mauz et al. (2012); Shennan et al. (2015)
Sediment facies	Shoreface: asymmetrical or symmetrical ripple lamination, high-angle cross beds, bioturbated beds of (bioclastic, carbonate, siliciclastic) well-sorted fine sand, seaward fining of grain size	Below MLW	Upper shoreface to inner shelf (ca -0.5 m to -8 m)	Miall (2010); Reading (1986); Shennan et al. (2015)
Cladocora caespitosa reef	Reef-like structure built by coral colony	MSL	Living range: 5-20 m water depth	Kruzic´ and Benkovic, (2008)

2.1 Marine Terrace

The marine terrace is a gently seaward dipping surface typically covered by a veneer of coastal sediment. It typically occurs on uplifting (and subsiding) coasts where the interaction between wave action, hard-rock lithology and sediment starvation allow a wave abrasion platform to form during sea-level highstand. Because the inner margin, located updip of the terrace deposit, is often buried by terrestrial sediments, reconstruction of the maximum shoreline position is a challenge and requires digital elevation model (DEM) analyses (e.g. Jara-Muñoz et al., 2016). In the eastern Mediterranean many of the marine terraces occur around the Aegean Sea as a result of ongoing deformation of the lithosphere at the Hellenic subduction zone (e.g., islands of Crete and Cyprus), along the North Anatolian transform fault (e.g., Marmara Sea), along the Kephalonia transform fault (southern Balkans) and along extensional faults (e.g. Gulf of Corinth, Antakya Graben). Because the terraces bear testimony to late Quaternary deformation history, they are often investigated in tectonic studies where dimension and elevation are constrained through DEM, DGPS and similar techniques and the timing of formation is deduced from radiometric dating of the terrace surface and deposits. Thus, as long as additional techniques (e.g., GPR) are not employed, the marine terrace is considered marine-limiting or it is a sea-level indicator with an uncertainty deduced from the DEM resolution (e.g., 5 m).

2.2 Sediment Facies

Eastern Mediterranean coastal sediments are represented by beach or fan-delta conglomerate, siliciclastic, carbonate and oolitic sand, clay and silt. These sediments may constitute beach ridges, barriers, veneers on terraces, beaches, lagoons or sabkhas resting in coastal onlap architecture on a flooding or erosional surface. A coastal deposit is undifferentiated and, hence, marine-limiting if the depositional environment has not been determined. It is considered a sea-level indicator where facies determination allows inferring water depth (Table 1). The indicative range of each sediment facies varies depending on the coastal topography, rate of sediment supply and prevailing hydrodynamics and must be determined for each site separately. With the small tidal range in the eastern Mediterranean the vertical precision of an index point deduced from sediment facies can be <50 cm in places. However, with the difficulty of dating, the number of high-quality facies-based indicators remains small.

2.3 *Cladocora Caespitosa* Reef

Cladocora caespitosa is a scleractinian polyp characterised by a corallite skeleton. It is a colonial coral species which forms banks of variable size on rocky and, occasionally, on sandy seabeds. The temperate coral is endemic to the Mediterranean where it shows relatively slow skeletal growth rates ranging from 1.3 mm yr^{-1} (Peirano et al., 2009) to 6.2 mm yr^{-1} (Kružic and Požar-Domac, 2003) mainly controlled by water temperature (Rodolfo-Metalpa et al., 2008). The colonies grow in shallow water and are rarely found below 30 m water depth (Kružić and Benkovic, 2008) and are therefore considered marine-limiting. Living and fossil *C. caespitosa* colonies are reported for north and central Aegean Sea, Marmara Sea, Crete, Cyprus, Levant, Gulf of Gabès, north Tunisia and Strait of Sicily (Ozalp and Alparslan, 2011). The coral has been used predominantly for the purpose of U-series dating the associated LIG deposits with limited success however, likely caused by the strong seawater temperature dependence (Trotter et al., 2011) and associated crystal instability of carbonate minerals secreted by the coral compared to their tropical counterparts.

3 Eastern Mediterranean LIG sea-level sites

In total 10 indicators are compiled and displayed against their longitudinal position in Fig. 2. When taking the uncertainty into account, the minimum and maximum LIG sea level is at -1.5 m and 23 m, respectively.

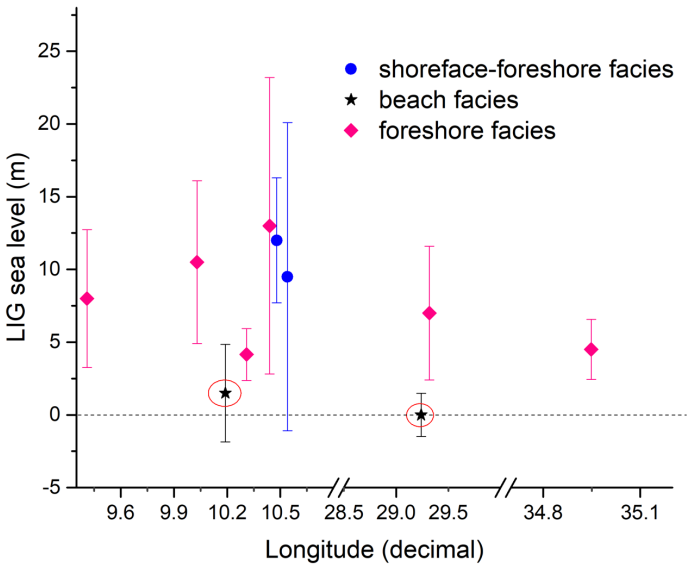

Fig. 2. The eastern Mediterranean sea-level indicators plotted against their longitudinal position. Red circle highlights datapoints potentially affected by non-GIA processes.

The 10 indicators displayed in Fig. 2 are situated on coastal zones affected by the interplay of eustacy and associated regional GIA only and provide age constraints and/or the Senegal fauna. Zones with minor or debated non-GIA contributions are also included. Coastal zones for which non-GIA processes during the late Quaternary are unambiguously evident are excluded (for zones see Fig. 1). For the selected zones we assume coastal geometries, hence tidal prism similar to today because the course of the LIG beach ridges and barriers suggest a LIG coastline running sub-parallel to the modern one. The tidal regime in the eastern Mediterranean is dominated by the equilibrium tide modified by the incoming Atlantic wave (Tsimplis et al., 1995). Generally, the mean tidal range today is 0.5 m (Admiralty Tide tables) apart from the Gulf of Gabès (1.5 m mean tidal range; Gzam et al., 2016). The mean tidal range is modified spatially by land-ocean distribution (e.g., northern Aegean Sea) and seasonally by ocean swell in winter.

3.1 Black Sea rift zone

Sile **(ID 927**; Fig. 1) – the around 80 cm thick cemented, moderately sorted bioclast-rich sand ("Coquinite"; Erginal et al. 2017) shows seaward dipping laminae in its lower part and tabular planar cross-beds in its upper part; depositional environment is foreshore to beach (Erginal et al., 2017). The deposit is situated at 0±1 m. Assuming a virtual absence of tides in the Black Sea (Medvedev et al., 2016) and an operational Bosporus gateway during LIG, this is a facies-based sea-level indicator with an indicative range of 0-2 m water depth. The palaeo-sea level is at 0.0±1.5 m at 127±9 ka (Erginal et al., 2017). The site is affected by subsidence estimated to ~2.3 mm/a for the most recent period (2008-2014) of the instrumental record (Avsar et al., 2017).

3.2 Nile littoral cell zone

Nahel Me'arot **(ID 3636**; Fig. 3) – the around 5 m thick deposit contains seaward dipping planar laminae of cemented oolitic grainstone; the depositional environment is lower foreshore to upper shoreface deduced from the modern analogue (Mauz et al., 2012). The elevation is 3-6 m (Galili et al., 2007). This is a facies-based sea-level indicator with an indicative range of 3-6 m water depth. The palaeo-sea level is at 4.5±2.1 m at 113±5 ka.

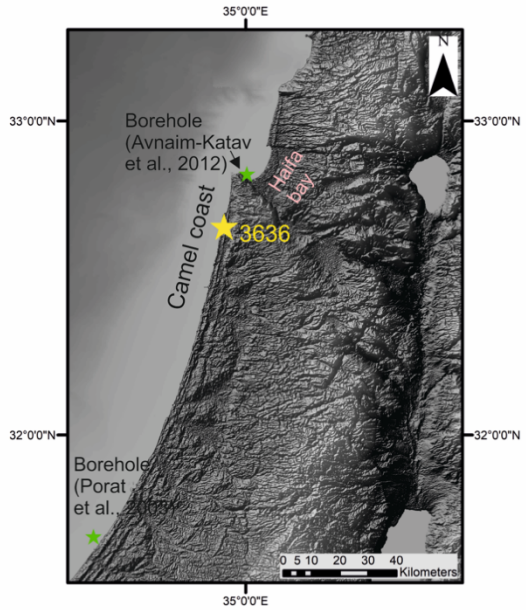

Fig. 3. The Levant Sea coast of Israel and the WALIS datapoint (ID 3636) situated on the Carmel coast. Green stars indicate location of boreholes. Gebco data were obtained from GEBCO Compilation Group (2020) GEBCO 2020 Grid (doi:10.5285/a29c5465-b138-234d-e053-6c86abc040b9). SRTM data were obtained from http://srtm.csi.cgiar.org (Jarvis et al., 2008).

3.3 African passive continental margin zone

El-Max-Abu Sir **(ID 1362**; Fig. 4) – The LIG shoreline is represented by the second beach ridge behind the modern coastline. Cross-bedded bioclastic and oolitic grainstone of foreshore depositional environment (Elshazly et al., 2019) constitute the basal part of the ridge. The elevation should be < 5 m but is poorly defined. This is a facies-based sea-level indicator with an indicative range of 1-3 m water depth. The palaeo-sea level is at 7±5 m at 121±6 ka (El-Asmar, 1994).

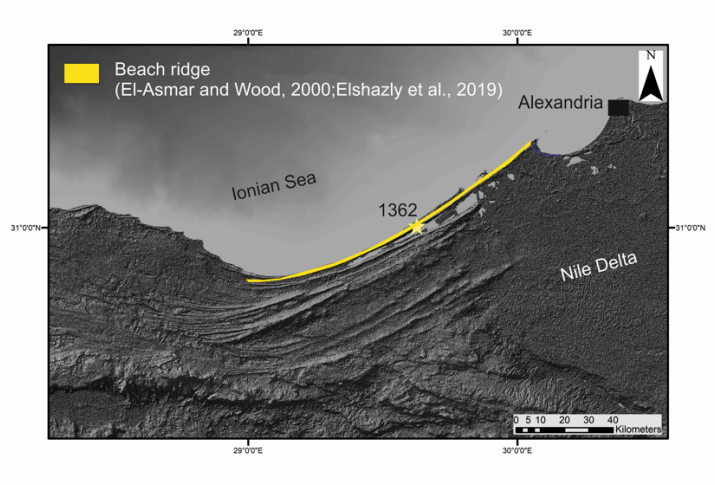

Fig. 4. The Ionian Sea coast west of the Nile delta (Egypt). The WALIS datapoint is ID 1362. Gebco data were obtained from GEBCO Compilation Group (2020) GEBCO 2020 Grid (doi:10.5285/a29c5465-b138-234d-e053-6c86abc040b9). SRTM data were obtained from http://srtm.csi.cgiar.org (Jarvis et al., 2008).

Ras Karboub **(ID 1363**; Fig. 5) – This site is part of the Jeffara barrier stretching almost parallel to the modern coastline from Sabratah (Libya) to Djerba island (Tunisia). The barrier shows siliciclastic sand of shoreface to foreshore gradually passing into oolitic grainstone of foreshore environment (Jedoui et al., 2003; Mauz et al., 2009). The elevation should be 5-10 m but is poorly defined. This is a facies-based sea-level indicator with an indicative range of 0.0 m to -3 m. The palaeo-sea level is at 9.5±10.6 m at 114±16 ka (Mauz et al., 2012).

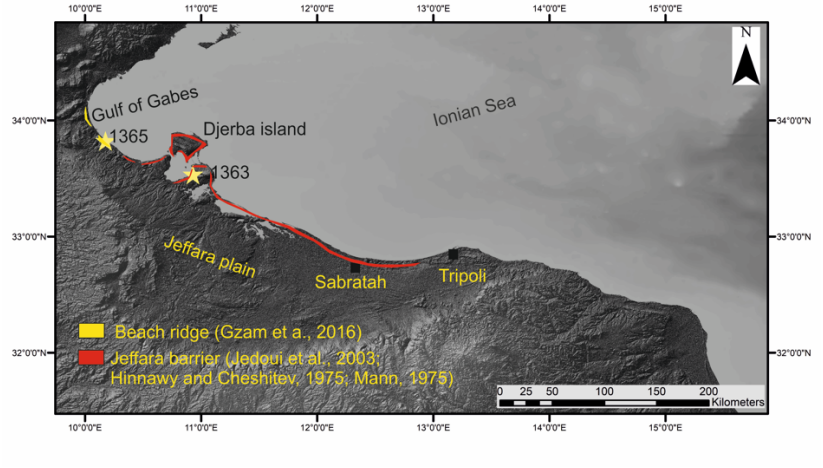

Fig. 5. The Ionian Sea coast between the Gulf of Sirte and the Gulf of Gabès (Libya and Tunisia) The datapoints included in the WALIS database are depicted with their WALIS ID. Gebco data were obtained from GEBCO Compilation Group (2020) GEBCO 2020 Grid (doi:10.5285/a29c5465-b138-234d-e053-6c86abc040b9). SRTM data were obtained from http://srtm.csi.cgiar.org (Jarvis et al., 2008).

***Khniss* (ID 1364**; Fig. 6) - This site is part of the Hammamet barrier stretching almost parallel to the modern coastline from Chebba to ID 926. The barrier shows siliciclastic sand of shoreface to foreshore environment gradually passing into oolitic grainstone of foreshore environment (Jedoui et al., 2003; Mauz et al., 2009). The elevation should be 5-10 m but is poorly defined. This is a facies-based sea-level indicator with an indicative range of +1m to -3 m. The palaeo-sea level is at 12±4 m at 121±10 ka (Mauz et al., 2009).

***Hergla* (ID 926**; Fig. 6) - the around 2 m thick cemented bioclastic quartz sand shows planar laminae; the depositional environment is foreshore (Mauz et al., 2018). The elevation of the corresponding shoreline should be at 3-2 m deduced from the altitude of the coeval lagoonal deposit (Mauz et al., 2018). This is a facies-based sea-level indicator with an indicative range of 1-3 m water depth. The palaeo-sea level is at 4.2±1.8 m at 120±5 ka.

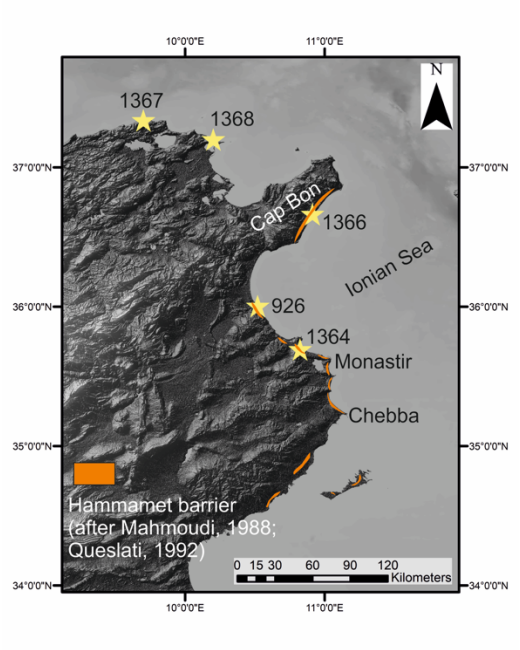

Fig. 6. The westernmost Ionian Sea coast (Tunisia). The datapoints included in the WALIS database are depicted with their WALIS ID. Gebco data were obtained from GEBCO Compilation Group (2020) GEBCO 2020 Grid (doi:10.5285/a29c5465-b138-234d-e053-6c86abc040b9). SRTM data were obtained from http://srtm.csi.cgiar.org (Jarvis et al., 2008).

3.4 Coastal lowlands

Gulf of Gabès **(ID 1365**; Fig. 5) – The LIG deposit is part of a coastline-parallel beach ridge. The lower part of the ridge is characterised by planar laminated beds of bioclastic sand bearing Strombus bubonius fossil remains (Gzam et al., 2016). The deposit is situated at 3 m (Gzam et al., 2016). This is a facies-based sea-level indicator with an indicative range of +0.5 m to 0 m including 1.5 m mean tidal range. The palaeo-sea level is at 1.5±3.4 m during MIS 5e.

3.5 Alpine orogenic belt

Korba **(ID 1366**; Fig 6) – This site is part of the Cap Bon barrier stretching almost parallel to the modern coastline (Elmejdoub and Jedoui 2009). The barrier shows siliciclastic sand in cross-bed or foreset bedding bearing Strombus bubonius in places (Elmejdoub and Jedoui 2009). The depositional environment is foreshore to beach (Elmejdoub and Jedoui, 2009; Mauz et al., 2012). The elevation should be 5-10 m but is poorly defined. This is a facies-based sea-level indicator with an indicative range of +1 m to -3 m. The palaeo-sea level is at 13±10 m during MIS 5e.

Rass Zebib **(ID 1368**; Fig. 6) – the indicator is part of a cliff section the lower part of which is characterised by planar laminated beds of bio- and siliciclastic sand of shoreface to foreshore environment (Mauz et al., 2009). The elevation should be around 5 m but is poorly defined. This is a facies-based sea-level indicator with an indicative range of -3 m to -8 m. The palaeo-sea level is at 11±6 m at 131±7 ka (Mauz et al., 2009).

Ras el Korane **(ID 1367**; Fig. 6) - the indicator is part of a cliff section the middle part of which is characterised by low-angle cross bedded bioclastic calcarenites (Sahli et al., 2019). The depositional environment is foreshore. The elevation should be 5-6 m but is poorly defined. This is a facies-based sea-level indicator with an indicative range of -1 m to -5 m. The palaeo-sea level is at 8±5 m during MIS 5e as deduced from facies correlation (Sahli et al., 2019).

4 Discussion

4.1 Quality of data

All sea-level indicators are facies-based and characterised by relatively small indicative ranges owing to the small tidal ranges on the respective coastal zones. The uncertainty of the indicator is high owing to poorly constrained elevation data. Because facies relationships and coastal architecture is also poorly defined in most sites, the indicators are generally of medium to low quality. There are two exception to this: the Nahel Me'arot site (ID 3636) and the Hergla site (ID 926). Both sites are characterised by well-understood facies architecture and facies relationship (Hearty et al., 2007; Galili et al., 2007; Mauz et al., 2012, 2018). The Hergla coastal barrier is situated at the modern coastline where it forms a cliff suggesting subsidence and/or effects of dynamic topography impacting on today's elevation of the former barrier. The Nahel Me'arot site is situated behind the modern coastline. The Holocene GIA model data suggest that the LIG sea-level position deduced from this site is of high quality (see below).

4.2 Impact of GIA mechanisms on the LIG shoreline elevation

The Mediterranean coast is a medium field relative to the former ice sheets and is therefore less sensitive to ice volume uncertainties. The Holocene modelling work indicates that some areas are relatively insensitive to earth-model parameter choice (Fig. 7; Lambeck et al., 2004; Lambeck and Purcell, 2005; Stocchi and Spada, 2007). Region 5 (Fig. 7) is suitable for sea-level reconstruction even if the predicted RSL deviates from the far-field eustatic curve because its insensitivity coincides with negligible surface deformation. Because parts of region 5 are affected by non-GIA deformation (e.g., Marmara Sea, Gulf of Sirte, Gulf of Gabès) suitable coastal zones in the eastern Mediterranean are located on the Levant coast and on the southern Ionian coast (Libya).

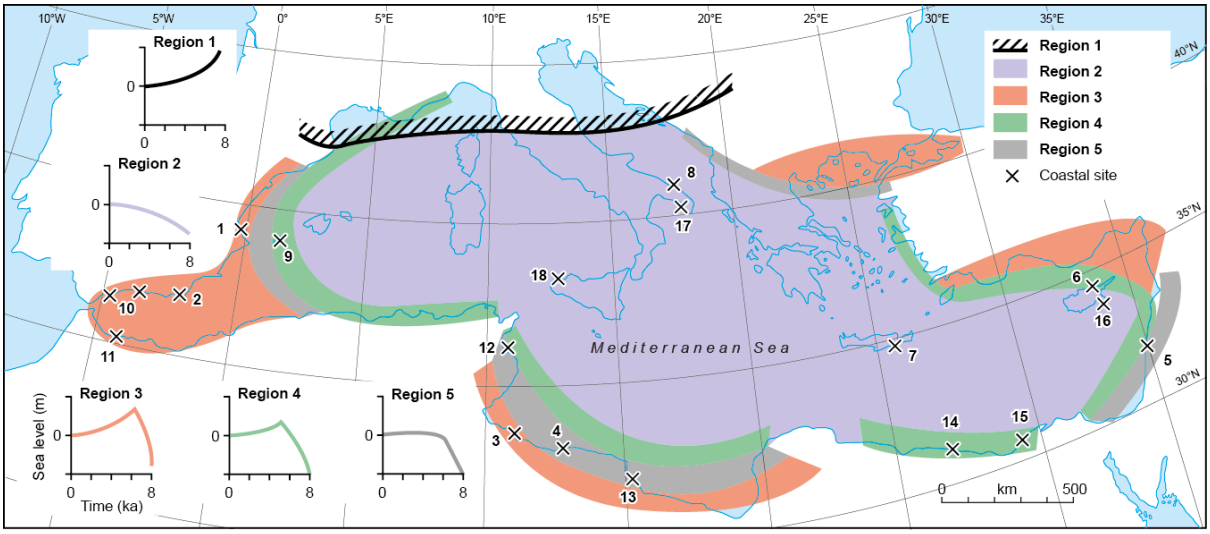

Fig. 7. RSL regions for t < 9 ka. Data are compiled from Lambeck and Purcell (2005) and Stocchi and Spada (2007) using ice models ICE3G, ICE5G, ICE1+A3, NE1, NE2, NA1, NA2. All models assume cessation of melting at 6 ka. Numbers indicate Holocene sites representing the corresponding RSL region.

Similar to other mid-latitudinal coastal areas (e.g., US-Carolina coast; Parham et al., 2007) controversies exist on the position of the MIS 5 shorelines. In fact, only few sites show the LIG shoreline at the commonly expected 6 m altitude (Fig. 2). Furthermore, for the MIS 5a Dorale et al. (2010) indicate that the shoreline in the West Mediterranean should have been close to modern MSL, but at Hergla (ID 926) the shoreline is at ~4 m (Mauz et al., 2018). Following results from geophysical modelling (e.g., Creveling et al., 2015) even the far-field shoreline can depart by up to 4 m from the eustatic value owing to local dynamic topography (e.g., Austermann et al., 2017). On the other hand, the LIG eustatic level is reconstructed probabilistically with a 4 m uncertainty (Kopp et al., 2013). Transferring these findings to the eastern Mediterranean, we can say that on tectonically dormant coasts the LIG sea level must have been situated at 5 ± 8 m. In fact, all our datapoints depicted in Fig. 2 fall in this range suggesting that reliable sites were selected in this review. The sites ID3636, 1362, 1363 and 1364 are in line with the GIA predictions for the Holocene. The mean LIG sea-level position deduced from these sites is 8.3±12.6 m. It is probable that this value is accurate but its precision requires more analytical effort regarding elevation and facies.

Acknowledgements

We thank Sara Stuecker (Salzburg) for generating the DEMs used for the map-based figures. Thanks also to Jenni Robertson for clarifying with us the altitude of the Crete terraces. The data described in this paper were compiled in WALIS, the sea-level database funded by ERC-StG-802414 (A Rovere et al.) and developed by the PALSEA working group (A Rovere, D Ryan, T Lorscheid, A Dutton, P Chutcharavan; D Brill, N Jankowski, D Mueller, M Bartz).

References

Admiralty Tide tables, available at https://www.admiralty.co.uk/digital-services/catalogues/admiralty-digital-catalogue.

Armijo, R., Meyer, B., King, G. C. P., Rigo, A., D. Papanatassiou, D.: Quaternary evolution of the Corinth Rift and its implications for the Late Cenozoic evolution of the Aegean. Geophys. J. Int. 126, 11-53, 1996.

Athanassis, C., Foutoulis, I.: Quaternary Neotectonic Configuration of the Southwestern Peloponnese, Greece, Based on Luminescence Ages of Marine Terraces. Journal of Earth Science, 24, No. 3, 410–427, DOI: 10.1007/s12583-013-0334-1, 2013.

Austermann, J., Jerry X. Mitrovica, Huybers, P. and Rovere, A.: Detection of a dynamic topography signal in last interglacial sea-level records. Science Advances 2017:3, e1700457, 2017.

Avnaim-Katav, S., Almogi-Labin, A., Sandler, A., Sivan, D., Porat, N. and Matmon, A.: The chronostratigraphy of a Quaternary sequence at the distal part of the Nile littoral cell, Haifa Bay, Israel. J. Quat. Sci. 27(7), 675-686, DOI: 10.1002/jqs.2537, 2012.

Avsar, N.B., Shuanggen Jin, S. Hakan Kutoglu, Gurbuz, G.: Vertical land motion along the Black Sea coast from satellite altimetry, tide gauges and GPS. Advances in Space Research 60, 2871–2881, http://dx.doi.org/10.1016/j.asr.2017.08.012, 2017.

Bialik, O.M., Frank, M., Betzler, C., Zammit, R. and Waldmann, N.D.: Two-step closure of the Miocene Indian Ocean Gateway to the Mediterranean. Sci. Reports 9:8842, https://doi.org/10.1038/s41598-019-45308-7, 2019.

Brew, G. Barazangi, M., Al-Maleh, A.K. and Sawaf, T.: Tectonic and Geologic Evolution of Syria. GeoArabia, 6, No. 4, 573-615, 2001.

Bulkan, S., Vannucchi, P., Gasperini, L., Polonia, A and Cavozzi, C.: Modelling tectonic deformation along the North-Anatolian Fault in the Sea of Marmara. Tectonophysics 794, 228612, https://doi.org/10.1016/j.tecto.2020.228612, 2020.

Collier, R.E.LL.: Eustatic and tectonic controls upon Quaternary coastal sedimentation in the Corinth Basin, Greece. Journal of the Geological Society, London, 147, 301-314, 1990.

Creveling, J., Jerry X. Mitrovica, Carling C. Hay, Jacqueline Austermann, Robert E. Kopp: Revisiting tectonic corrections applied to Pleistocene sea-level highstands. Quat. Sci. Rev. 111, 72-80, http://dx.doi.org/10.1016/j.quascirev.2015.01.003, 2015.

Davis, M., Matmon, A., Root, D.H. and Avnaim-Katav, S.: Constant cosmogenic nuclide concentrations in sand supplied from the Nile River over the past 2.5 m.y. Geology, doi:10.1130/G32574.1, 2012.

De Gelder, G., Fernández-Blanco, D., Melnick, D., Duclaux, G., Bell, R.E., Jara-Muñoz, J., Armijo, R., Lacassin, R.: Lithospheric flexure and rheology determined by climate cycle markers in the Corinth Rift. Sci. Reports, https://doi.org/10.1038/s41598-018-36377-1, 2019.

Dodonov, A. E., Trifonov, V. G., Ivanova, T. P., Kuznetsov, V. Y., Maksimov, F. E., Bachmanov, D. M., Sadchikova, A.N., Minini, H., Al-Kafri, A.-M. and Ali, O.: Late Quaternary marine terraces in the Mediterranean coastal area of Syria: Geochronology and neotectonics. Quat. Int. 190(1), 158-170, doi:10.1016/j.quaint.2008.02.008, 2008.

Dorale, J.A., Onac, B.P., Fornos, J.J., Gines, J., Gines, A., Tuccimei, P., Peate, D.W.: Sea-level highstand 81,000 years ago in Mallorca. Science 327, 860-863, 10.1126/science.1181725, 2010.

El-Asmar, H.M., 1994. Aeolianite sedimentation along the northwestern coast of Egypt: Evidence for middle to late Quaternary aridity. Quaternary Science Reviews 13, 699-708, 1994.

El-Asmar, H.M., and Wood, P.: Quaternary shoreline development: the northwestern coast of Egypt: Quaternary Science Reviews 19, 1137-1149, 2000.

Elmejdoub, N. and Jedoui, Y.: Pleistocene raised marine deposits of the Cap Bon peninsula (N–E Tunisia): Records of sea-level highstands, climatic changes and coastal uplift. Geomorphology 112, 179-189, doi:10.1016/j.geomorph.2009.06.001, 2009.

Elshazly, A., El-Sayed, M.K. and Pascucci, V.: A sedimentary depositional and diagenetic model of a Pleistocene/Holocene coastal formation in Alexandria, Mediterranean Sea, Egypt. J. Afr. Earth Sci. 158, 103552, https://doi.org/10.1016/j.jafrearsci.2019.103552, 2019.

Emery, K.O., Neev, D.: Mediterranean beaches of Israel. Bulletin Geological Survey Israel 26, 1–23, 1960.

Erginal, A.E., Nafiye Güne. Kıyak, Hamit Haluk Selim, Mustafa Bozcu, Muhammed Zeynel .ztürk, Yunus Levent Ekinci, Alper Demirci, Elmas Kırcı Elmas, Tug˘ba .ztürk, Çag˘lar Çakır, Mustafa Karabıyıkog˘lu: Eolianite and coquinite as evidence of MIS 6 and 5, NW Black Sea coast, Turkey. Aeolian Research 25, 1-9, http://dx.doi.org/10.1016/j.aeolia.2017.01.004, 2017.

Galili, E., Zviely, D., Ronen, A., Mienis, H.K.: Beach deposits of MIS 5e high sea stand as indicators for tectonic stability of the Carmel coastal plain. Israel. Quaternary Science Review, 26, 2544-2557, 2007.

Galili, E., Sevketoglu, M., Salamon, A., Zviely, D., Mienis, H.K., Rosen, B. and Moshkovitz, S.: Late Quaternary beach deposits and archaeological relicts on the coasts of Cyprus, and the possible implications of sea-level changes and tectonics on the early populations, in: Geology and Archaeology: Submerged Landscapes of the Continental Shelf, edited by: Harff, J., Bailey, G. and Luth, F., Geological Society, London, Special Publications, 411, 179–218, http://dx.doi.org/10.1144/SP411.10, 2016.

Galili, E., Ronen, A., Mienis, H.K. and Horwitz, L.K.: Beach deposits containing middle Paleolithic archaeological remains from northern Israel. Quat. Int. 464, 43-57, http://dx.doi.org/10.1016/j.quaint.2017.05.002, 2018.

Gallen, S.F., K.W. Wegmann, D.R. Bohnenstiehl, F.J. Pazzaglia, M.T. Brandon, C. Fassoulas: Active simultaneous uplift and margin-normal extension in a forearc high, Crete, Greece. Earth Plan. Sci. Lett. 398, 11-24, http://dx.doi.org/10.1016/j.epsl.2014.04.0380012-821X, 2014.

Gawthorpe, R.L., Leeder, M.R., Kranis, H., Skourtsos, E., Andrews, J.E., Gijs A. Henstra, Greg H. Mack, Martin Muravchik, Jenni A. Turner, Michael Stamatakis: Tectono-sedimentary evolution of the Plio-Pleistocene Corinth rift, Greece. Basin Research 30, 448-479, doi: 10.1111/bre.12260, 2018.

Gharbi, M., Bellier, O., Masrouhi, A., Espurt N.: Recent spatial and temporal changes in the stress regime along thesouthern Tunisian Atlas front and the Gulf of Gabes: New insightsfrom fault kinematics analysis and seismic profiles. Tectonophysics 626, 120-136, http://dx.doi.org/10.1016/j.tecto.2014.04.003, 2014.

Gibbard, P., Cohen, K.: Global chronostratigraphical correlation table for the last 2.7 million years. Episodes 31, 243-247, 2008.

Giglia, G.: Explanatory Booklet, Sheet: Ajdabiya, NH 34-6. Geological map of Libya. Industrial research Centre Tarabulus, Centro Ricerche Geologiche S.p.A., Firence, Italy, p. 1-93, 1984.

Gignoux, M.: Les formations marines Pliocènes et Quaternaires de l′Italie du sud et de la Sicile. Ann. d. L′Univ.Lyon N. S., 36, 1913.

Granot, R.: Palaeozoic oceanic crust preserved beneath the eastern Mediterranean. Nat. Geosci., DOI: 10.1038/NGEO2784, 2016.

Gzam, M., Elmejdoub, N. and Jedoui, Y.: Late Quaternary sea level changes of Gabes coastal plain and shelf: Identification of the MIS 5c and MIS 5a onshore highstands, southern Mediterranean. J. Earth Syst. Sci. 125, No 1, 13-28, 2016.

Hafkenscheid, E., Wortel, M.J.R. and Spakman, W.: Subduction history of the Tethyan region derived from seismic tomography and tectonic reconstructions. J. Geophys. Res. 111, B08401, doi:10.1029/2005JB003791, 2006.

Hearty, P.J.: An inventory of last interglazial (sensu lato) age deposits from the Mediterranean basin: a study of isoleucine epimerisation and U-Series dating. Zeitschrift fur Geomorphologie, Supplementum 62, 51–69, 1986.

Hearty, P.J., Hollin, J.T., Neumann, A.C., O'Leary, M.J., McCulloch, M.: Global sea- level fluctuations during the Last Interglaciation (MIS 5e). Quaternary Science Reviews 26, 2090-2112, 2007.

El-Hinnawy, M. and Cheshitev, G.: Explanatory Booklet, Sheet: Tarabulus, NI 33-13. Geological map of Libya. Libyan Arab Republic, Industrial research Centre, p. 1-55, 1975.

Issar, A., and Kafri, U.: Neogene and Pleistocene geology of the Western Galilee coastal plain, Geological Survey of Israel Bulletin 53**,** 1–14, 1972.

Jara- Muñoz, J., Melnick, D., Strecker, M.R.: TerraceM: A MATLAB® tool to analyze marine and lacustrine terraces using high-resolution topography. Geosphere 12(1), 176-195, doi:10.1130/GES01208.1, 2016.

Jarvis, A., H.I. Reuter, A. Nelson, E. Guevara,: Hole-filled SRTM for the globe Version 4, available from the CGIAR-CSI SRTM 90m Database http://srtm.csi.cgiar.org, 2008

Jedoui, Y., Reyss, J.-L., Kallel, N., Montacer, M., Ismaïl, H.B., Davaud, E.: U-series evidence for two high Last Interglacial sea levels in southeastern Tunisia. Quaternary Science Reviews 22, 343-351 2003.

Jenkins, J., Stephenson, S.N., Martinez-Garzon, P., Bohnhoff, M. and Nurlu, M.: Crustal Thickness Variation Across the Sea of Marmara Region, NW Turkey: A Reflection of Modern and Ancient Tectonic Processes. Tectonics 39, e2019TC005986. https://doi.org/10.1029/2019TC005986, 2020.

Keraudren, B., Sorel, D.: The terraces of Corinth (Greece) A detailed record of eustatic sea-level variations during the last 500,000 years. Mar. Geol. 77, 99-107, 1987.

Kopp, R.E., Simons, F.J., Mitrovica, J.X., Maloof, A.C. and Oppenheimer, M.: Probabilistic assessment of sea level during the last interglacial stage. Nature 462, 863-868, doi:10.1038/nature08686, 2009.

Kopp, R.E., Frederik J. Simons, Jerry X. Mitrovica, Adam C. Maloof, Michael Oppenheimer: A probabilistic assessment of sea level variations within the last interglacial stage. Geophys. J. Int. 193, 711–716, doi: 10.1093/gji/ggt029, 2013.

Kružic, P., Benkovic, L.: Bioconstructional features of the coral Cladocora caespitose (Anthozoa, Scleractinia) in the Adriatic Sea (Croatia). Marine Ecology 29, 125-139, doi:10.1111/j.1439-0485.2008.00220.x, 2008.

Kružic, P., Požar-Domac, A.: Banks of the coral Cladocora caespitose (Anthozoa, Scleractinia) in the Adriatic Sea. Coral Reef 22, 536, DOI 10.1007/s00338-003-0345-y, 2003.

Lambeck, K., Antonioli, F., Purcell, A., Silenzi, S.: Sea-level change along the Italian coast for the past 10,000 yr. Quat. Sci. Rev. 23, 1567-1598, doi:10.1016/j.quascirev.2004.02.009, 2004.

Lambeck, K. and Purcell, A.: Sea-level change in the Mediterranean Sea since the LGM: model predictopns for tectonically stable areas. Quat. Sci. Rev. 24, 1969-1988, doi:10.1016/j.quascirev.2004.06.025, 2005.

Mahmoudi, M.: Nouvelle proposition de subdivisions stratigraphiques des depots attribues au Tyrrhenien en Tunesie (region de Monastir). Bull. Soc. Geol. France 8(3), 431-435., 1988.

Mann, K.: Explanatory Booklet, Sheet: Al Khums, NI 33-14. Geological map of Libya. Libyan Arab Republic, Industrial research Centre Tripoli, p. 1-80, 1975.

Mauz, B., Elmejdoub, N., Nathan, R., Jedoui, Y.: Last interglacial coastal environments in the Mediterranean–Sahara transition zone. Palaeogeography, Palaeoclimatology, Palaeoecology 279, 137–146, https://doi.org/10.1016/j.palaeo.2009.05.006, 2009.

Mauz, B., Fanelli, F, Elmejdoub, N. and Barbieri, R.: Coastal response to climate change: Mediterranean shorelines during the last interglacial (MIS 5). Quaternary Science Reviews 54, 89-98, doi:10.1016/j.quascirev.2012.02.021, 2012.

Mauz, B., Shen, Z., Elmejdoub, N. and Spada, G.: No evidence from the eastern Mediterranean for an MIS 5e double peak sea-level highstand. Quaternary Research, 1-6 doi:10.1017/qua.2017.111, 2018.

Mauz, B.: Database of last interglacial sea-level proxies in the eastern Mediterranean [Data set]. Zenodo, http://doi.org/10.5281/zenodo.4454553, 2020.

McNeill, L.C., Donna J. Shillington, Gareth D. O. Carter, Jeremy D. Everest, Robert L. Gawthorpe, Clint Miller, Marcie P. Phillips, Richard E., Ll. Collier, Aleksandra Cvetkoska, Gino De Gelder, Paula Diz, Mai-Linh Doan, Mary Ford, Maria Geraga, Jack Gillespie, Romain Hemelsdaël, Emilio Herrero-Bervera, Mohammad Ismaiel, Liliane Janikian, Katerina Kouli, Erwan Le Ber, Shunli Li, Marco Maffione, Carol Mahoney, Malka L. Machlus Georgios Michas, Casey W. Nixon, Sabire Asli Oflaz, Abah P . Omale, Kostas Panagiotopoulos, Sofia Pechlivanidou, Simone Sauer, Joana Seguin, Spyros Sergiou, Natalia V. Zakharova, Sophie Green: High-resolution record reveals climate-driven environmental and sedimentary changes in an active rift. Scientific Reports, https://doi.org/10.1038/s41598-019-40022-w, 2018.

McPhee, P., van Hinsbergen, D.J.J.: Tectonic reconstruction of Cyprus reveals Late Miocene continental collision of Africa and Anatolia. Gondwana Research 68, 158-173, https://doi.org/10.1016/j.gr.2018.10.015, 2019.

Medvedev, I.P., Rabinovich, A.B. and Kullkov, E.A.: Tides in three enclosed basins: The Baltic, Black, and Caspian Seas. Front. Mar. Sci. 3:46. doi: 10.3389/fmars.2016.00046, 2016.

Miall, A.D.: The geology of stratigraphic sequences. Springer-Verlag Berlin Heidelberg, DOI: 10.1007/978-3-642-05027-5, 2010.

Morhange, C., Pirazzoli, P.A., Marriner, N., Montaggioni, L.F. and Nammour, T.: Late Holocene sea-level changes in Lebanon, Eastern Mediterranean. Mar. Geol. 230, 99-114, doi:10.1016/j.margeo.2006.04.003, 2006.

Nocquet, J.-M.: Present-day kinematics of the Mediterranean: A comprehensive overview of GPS results. Tectonophysics 579, 220-242, doi:10.1016/j.tecto.2012.03.037, 2012.

Ott, R.F., Gallen, S.F., Wegmann, K.W., Biswas, R.H., Herman, F. and Willett, S.D.: Pleistocene terrace formation, Quaternary rock uplift rates and geodynamics of the Hellenic Subduction Zone revealed from dating of paleoshorelines on Crete, Greece. Earth Plan. Sci. Lett. 525, 115757, https://doi.org/10.1016/j.epsl.2019.115757, 2019.

Ozalp, H.B., Alparslan, M.: Scleractinian diversity in the Dardanelles and Marmara Sea (Turkey): morphology, ecology and distributional patterns. Oceanological and Hydrobiological Studies 45, 259-285, DOI: 10.1515/ohs-2016-0023, 2016.

Palamakumbura, R. N., Robertson, A. H., Kinnaird, T. C., van Calsteren, P., Kroon, D.,and Tait, J. A.: Quantitative dating of Pleistocene deposits of the Kyrenia Range, northern Cyprus: implications for timing, rates of uplift and driving mechanisms. Journal of the Geological Society, 173(6), 933-948, doi:10.1144/jgs2015-130, 2016.

Parham, P.R., Riggs, S.R., Culver, S.J., Mallinson, D.J., Wehmiller, J.F.: Quaternary depositional patterns and sea-lever fluctuations, northeastern North Carolina. Quat. Res. 67, 83-99, doi:10.1016/j.yqres.2006.07.003, 2007.

Paskoff, R., Sanlaville, P., 1983. Les côtes de la Tunisie. Variations du niveau marin depuis le Tyrrénien. Coll. Maison de l'Orient, Lyon. 14, 192p.

Peirano, A., Kružić, P., Mastronuzzi, G.: Growth of Mediterranean reef of Cladocora caespitosa (L.) in the Late Quaternary and climate inferences. Facies 55, 325-333, DOI 10.1007/s10347-008-0177-x, 2009.

Poole A.J., and Robertson, A.H.F.: Quaternary uplift and sea-level changes at active plate boundary, Cyprus, Journal of Geological Society, London 148, 909-921, 1991.

Poole, A.J., Robertson, A.H.F., and Shimmield, G.: Late Quaternary uplift of the Troodos ophiolite, Cyprus; Uranium-series dating of Pleistocene coral. Geology 18, 894-897, 1990.

Porat, N., Avital, A., Frechen, M. and Almogi-Labin, A.: Chronology of upper Quaternary offshore successions from the southeastern Mediterranean Sea, Israel. Quat. Sci. Rev. 22, 1191-1199, doi:10.1016/S0277-3791(03)00016-7, 2003.

Queslati, A.:Salt marshes in the Gulf of Gabes (southeastern Tunisia): Their morphology and recent dynamics. J. Coast. Res. 8(3), 727-733, 1992.

Reading, H.G.: Sedimentary environments and facies. Blackwell Scientific Publications, London, 1986.

Robertson, J., M. Meschis, G. P. Roberts, A. Ganas, D. M. Gheorghiu: Temporally constant Quaternary uplift rates and their relationship with extensional upper-plate faults in south Crete (Greece), constrained with ^{36}Cl cosmogenic exposure dating. Tectonics 38, 1189-1222, DOI:10.1029/2018TC005410, 2019.

Rodolfo-Metalpa, R., Peirano A. F. Houlbreque, M., Abbate, C., Ferrier-Pages: Effects of temperature, light and heterotrophy on the growth rate and budding of the temperate coral *Cladocora caespitose*. Coral Reefs 27, 17-25, DOI 10.1007/s00338-007-0283-1, 2008.

Rovere, A. Raymo, M.E., Vacchi, M., Lorscheid, T., Stocchi, P., Gomez-Pujol, L., Harris, D.L., Casella, E., O'Leary, M.J. and Hearty, P.: The analysis of Last Interglacial (MIS 5e) relative sea-level indicators: Reconstructing sea level in a warmer world. Earth-Sci. Rev. 159, 404-427, http://dx.doi.org/10.1016/j.earscirev.2016.06.006, 2016.

Sahli, W., Saadi, J. and Regaya, K.: Sedimentology and high-frequency cycles of the late Pleistocene of the Bizerte area (N-E Tunisia). Arab. J. of Geosci., https://doi.org/10.1007/s12517-019-4719-z, 2019.

Sammari C, Koutitonsky V. G. and Moussa M.: Sea level variability and tidal resonance in the Gulf of Gabes, Tunisia; Continental Shelf Research 26**,** 338–350, 2006.

Sessa, J.A., Callapez, P.M., Dinis, P.A., Hendy, A.J.W.: Paleoenvironmental and paleobiogeographical implications of a middle Pleistocene mollusc assemblage from the marine terraces of Baía das Pipas, Southwest Angola. J Paleont. 87(6), 1016-1040, D1016S03.00 DOI: 10.1666/12-119, 2013.

Shennan, I.: Flandrian sea-level changes in the Fenland. II: tendencies of sea-level movement, altitudinal changes, and local and regional factors. J. Quat. Sci.1, 155-179, https://doi.org/10.1002/jqs.3390010205, 1986.

Shennan, I., Long, A.J., Horton, B.P. (Eds,), Handbook of sea-level research. John Wiley & Sons, Ltd, Chichester, 2015.

Sivan D., Sisma-Ventura G., Greenbaum N., Bialik O.M., Williams, F.H., Tamisiea, M.E., Rohling, E.J., Frumkin, A., Avnaim-Katav S., Shtienberg G., Stein M.: Eastern Mediterranean sea levels through the last interglacial from a coastal-marine sequence in northern Israel. Quaternary Science Reviews 145, 204-225, http://dx.doi.org/10.1016/j.quascirev.2016.06.001, 2016.

Sivan, D., Gvirtzman, G. and Sass, E.: Quaternary Stratigraphy and Paleogeography of the Galilee Coastal Plain, Israel. Quaternary Research 51, 280–294, qres.1999.2044, 1999.

Stocchi, P. and Spada, G.: Glacio- and hydro-isostasy in the Mediterranean Sea: Clark's zones and role of remote ice sheets, Annals of Geophysics 50(6), 2007.

Tari, U., Okan Tüysüz, Bonnie A.B. Blackwell, Zarrin Mahmud, Jonathan A. Florentin, Justin Qi, Ş. Can Genç, Anne R. Skinner: Seal level change and tectonic uplift from dated marine terraces along the eastern Mediterranean coast, southeastern Turkey. Palaeo-3 511, 80-102, https://doi.org/10.1016/j.palaeo.2018.07.003, 2018.

Trotter, J., Montagna, P., McCulloch, M., Silenzi, S., Reynaud, S., Mortimer, G., Martin, S., Ferrier-Pagès, C., Gattuso, J.-P. and Rodolfo-Metalpa, R.: Quantifying the pH 'vital effect' in the temperate zooxanthellate coral *Cladocora caespitosa*: Validation of the boron seawater pH proxy. Earth Plan. Sci. Lett. 303, 163-173, doi:10.1016/j.epsl.2011.01.030, 2011.

Tsimplis, N.M., Proctor, R. and Flather, A.: A two-dimensional tidal model for the Mediterranean Sea. J. Geophys. Res. 100 (C8), 16223-16239, 1995

van de Plassche, O. (ed): Sea-level research: A Manual for the collection and evaluation of data. Geo Books, Norwich, 1986.

van der Meer, F. and Cloetingh, S.: Intraplate stresses and the subsidence history of the Sirte Basin (Libya). Tectonophysics 226, 37-58, 1993.

Vita-Finzi, C.: ^{14}C dating of Late Quaternary uplift in western Cyprus. Tectonophysics, 172, 135–140 1990.

Vita-Finzi, C.: Evaluating Late Quaternary uplift in Greece and Cyprus. In: Prichard, H. M., Alabaster, T., Harris, N. B.W. and Neary, C. R. (eds), Magmatic Processes and Plate Tectonics. Geological Society, London, Special Publications, 76, 417–424, http://doi.org/10.1144/GSL.SP.1993.076.01.21, 1993.

Weinberger, R., Gross, M.R. and Sneh, A.: Evolving deformation along a transform plate boundary: Example from the Dead Sea Fault in northern Israel. Tectonics 28, TC5005, doi:10.1029/2008TC002316, 2009.

Yaltirak, C., Sakinc, M., Aksu, A.E., Hiscott, R.N., Galleb, B. and Ulgen, U.B.: Late Pleistocene uplift history along the southwestern Marmara Sea determined from raised coastal deposits and global sea-level variations. Mar. Geol. 190, 283-305.

Zomeni, Z.: Quaternary Marine Terraces on Cyprus: Constraints on Uplift and Pedogenesis, and the Geoarchaeology of Palaipafos. PhD thesis, Oregon State University, https://ir.library.oregonstate.edu/concern/graduate_thesis_or_dissertations/z603r1518?locale=en, 2012.

Zviely, D., Sivan, D., Ecker, A., Bakler, N., Rohrlich, V., Galili, E., Boaretto, E., Klein, M. and Kit, E.: Holocene evolution of the Haifa Bay area, Israel, and its influence on ancient tell settlements. The Holocene 16(6), 849-861, 10.1191/0959683606hol977rp, 2006.

An earlier version of this manuscript was submitted for publication in Earth System Science Data, Special Issue "WALIS – the World Atlas for Last Interglacial Shorelines", edited by A Rovere et al. It was reviewed and subsequently withdrawn by the corresponding author. For reference see https://doi.org/10.5194/essd-2020-357.